

Inelastic buckling and post-buckling behavior of gusset plate connections

Mohammad Ali Hadianfard ^{*1} and Ali Reza Khakzad ^{2a}

¹ Department of Civil and Environmental Engineering,
Shiraz University of Technology, P.O. Box 71555-313 Shiraz, Iran
² Eram Higher Education Institute, Shiraz, Iran

(Received February 04, 2016, Revised June 14, 2016, Accepted October 13, 2016)

Abstract. In this study, by using finite element non-linear static analysis and comparing it with experimental models, the buckling and post-buckling behavior of bracing gusset plates has been investigated. The effects of such parameters as dimension and thickness of the gusset plate and the influence of position of the bracing member on the behavior of gusset plate have been examined. The results of the analyses clearly suggest that capacity, buckling and post-buckling behaviors of gusset plates depend on the position of the bracing splice plate with respect to the free bending line as well as on the size and thickness of the gusset plate. Also, with respect to numerical analysis results, some practical graphs for the calculation of buckling capacity of gusset plate connections are presented. For steel structures, the proposed method is apparently more accurate than available code procedures.

Keywords: steel structures; gusset plate; bracing splice plate; buckling; post-buckling; free bending line

1. Introduction

Due to good stiffness and high resistance of braced steel frames, they have been widely used in seismic design of steel structures and have a very important role in attraction and dissipation of earthquake energy (Chen and Chang 2012, Güneysi and Ameen 2014, Bazzaz *et al.* 2012). Significant attention should be paid to bracing connections in steel structures due to whose complicated behavior. Insufficient knowledge about operation of bracing gusset plates may lead to improper design of these connections. The results of experimental tests and also finite element and finite difference models can aid to investigate strength and behavior of these plates (Lutz and LaBoube 2005, Rajasekaran and Wilson 2013, Naghipour *et al.* 2013, Hadianfard *et al.* 2015).

Because of complicated behavior of corner gusset plates in the centric bracing frames, the design procedure of these plates has been widely simplified in such methods as Whitmore (1952) and Thornton (1984).

In the Whitmore method (Whitmore 1952) for determining plate buckling load, an equivalent column is defined on gusset plate and the buckling load of gusset plate is considered to be equal to the buckling capacity of this equivalent column. Whitmore proposed the effective width for

*Corresponding author, Associate Professor, E-mail: hadianfard@sutech.ac.ir

^aM.Sc. Engineer, E-mail: alikh_ede@yahoo.com

determining the loading capacity of the gusset plate in which load distribution is based on an angle of 30 degrees. In the Thornton method (Thornton 1984), the buckling load of gusset plate is considered to be equal to the compressive strength of column strip with fixed-end supports under the Whitmore effective width. The overall view of gusset plate and parameters related to Whitmore and Thornton methods are respectively illustrated in Fig. 1 and Fig. 2. In Thornton's method, the length of column strip (L_c), as shown in Fig 2, is equal to the maximum of L_1 , L_2 and L_3 . The effective length factor for column strip is equal to $K = 0.65$. AISC-LRFD (2001) has used Thornton's method for estimating the ultimate load of gusset plates under compressive force P_{cr} . Gross (1990) suggested a method similar to that of Thornton but with a different effective length factor, $k = 0.5$, for determining compressive capacity. In the studies conducted by Astaneh-Asl (1998), for when the end of the bracing moves toward the outside of the plane, the conservative amount of $k = 1.2$ was suggested. Yam and Cheng (1993, 2002) for considering the effect of redistribution of load in the compressive gusset plate suggested the modified Thornton method with a correction in emission angle of 45 degrees instead of 30 degrees for determining column effective width. Comparing the results of Yam and Cheng, experiments with modified Thornton method show that this method compared to the original Thornton method calculates the ultimate load of the gusset plate with more accuracy. Also, effects of some parameters such as the thickness and dimension of the gusset plate, bracing angle, etc. on the strength and behavior of compressive gusset plates are considered in the supplementary experiments of Yam and Cheng (1993, 2002). Sheng *et al.* (2002) provided a new design method based on the inelastic critical buckling stress of plates instead of using column buckling equation for estimating plate ultimate load. The results showed that the ultimate load of the models decreases with increase in the free edge length of gusset plate (see Fig. 1), and the free edge length has a very effective influence on buckling strength of thin plates. Rabinovitch and Cheng (1993) studied cyclic behavior of steel gusset plates and effects of some parameters such as edge stiffeners on their performance. They examined tension and compression capacities of gusset plates by experimental investigation of full-scale connections. Wallbridge *et al.* (1998) studied the initial imperfection on buckling behavior of gusset plates and showed that by decreasing the amount of initial imperfection, the buckling behavior of the gusset plate improves. In the studies conducted by Hashemi *et al.* (2008), the effects of connection eccentricity were considered, and, for improving the buckling behavior of bracing gusset plates, bracings were suggested to be connected without any eccentricity. Roeder *et*

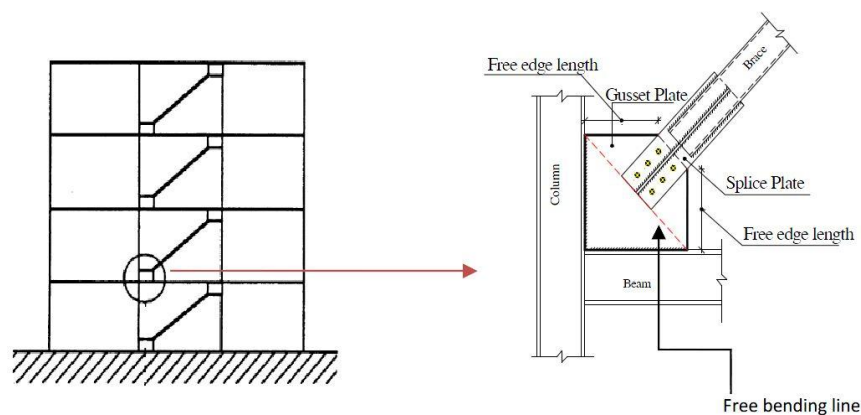


Fig. 1 View of the corner gusset plate

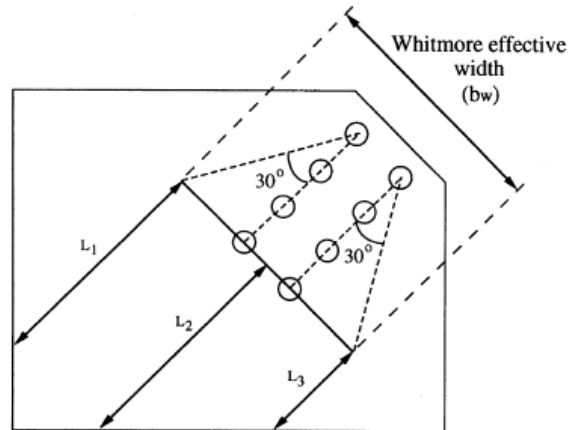


Fig. 2 Effective width of Whitmore and Thornton

al. (2004) and Lehman *et al.* (2008) showed that big and thick gusset plates cause concentration of deformation in the middle section of the plate and hence decrease ductility. Crosti and Duthinh (2014) proposed a nonlinear model for gusset plate connections of truss bridges. The proposed model provides a simple and affordable way to account for connection performance in global analysis. Fang *et al.* (2015) presented experimental, numerical, and analytical investigations of the compressive strength and behavior of gusset plate connections with single-sided splice members. Hassan *et al.* (2014), through an experimental program, studied the performance and behavior of different types of connections between circular concrete filled steel tube columns (CCFT) and gusset plates subjected to shear and axial compression loadings. Deliktas and Mizamkhan (2014) focused on finite element modeling of nonlinear behavior of the gusset plates of the truss based bridges subjected to dynamics loads. This study indicated the location of damage initiation in the gusset plate.

As is clear, a lot of research has been focused on buckling capacity and behavior of gusset plate connections, but seldom have the post-buckling behavior (unlike columns, gusset plates continue to carry loads even after buckling in a stable manner), position of bracing and the way it stands on the gusset plate been studied. Although the ability of methods presented by Whitmore and Thornton has been accepted, the results of this study indicate that the safety factors in using them are different. Furthermore, the method provided by Sheng *et al.* (2002) is usable for plates of some special dimensions and thicknesses. Therefore, in this research by considering gusset plates of different dimensions and analyzing different models in the Abaqus finite element software, the buckling and post-buckling behavior of gusset plates have been discussed and then by calculating the buckling load, design diagrams for different dimensions and thicknesses are presented. These diagrams depend on the position of the brace splice plate with respect to the free bending line (the line joining two corners of the gusset plate as shown in Fig. 2. Also it can be named as restrain line).

Another comparison done in this paper was between numerical analysis and the three methods of Whitmore (1952), Thornton (1984) and Modified Thornton (Yam and Cheng 1993). To verify the accuracy of the modeling, results of numerical analyses were compared with those of Yam and Cheng's (2002) laboratory model. In addition, dimensions and thicknesses of the gusset plates used in this study are selected as conventional plates in building construction.

2. Modeling

For the numerical study, a corner gusset plate of bracing was considered. The structural system was intermediate simple frame with concentric bracing and compatibility of inelastic rotation due to post-buckling deformation of gusset plates was neglected. In the model, the end of the diagonal member of the bracing can pass the free bending line (AISC 2005). The primary design of structure was based on Iranian earthquake code. The braces sections were selected on the basis of conventional construction in Iran. Also the geometry of the connections and primary dimensions of gusset plates were almost similar to Yam and Cheng (1993, 2002). The gusset plate has been supposed to be welded to the beam and column while connected to the bracing using a splice plate with bolted connections. The connection of the splice plate with the bracing is provided by welding (Fig. 3). Yielding and ultimate stresses, elastic modulus and Poisson's ratio of the plates are 360 MPa, 470 MPa, 210000 MPa and 0.3, respectively. The non-linear stress-strain diagram of steel is estimated to be bilinear. All materials used in modeling were isotropic. For the non-linear static analysis, Abaqus finite element software can be used. In Fig. 3, the position of bracing splice plate has been shown relative to the free bending line. The position of the splice plate in model (1) is before the free bending line, in Model (2) on the free bending line and in model (3) after the free bending line. The sections of all bracings are 2UNP140, and the sections of all beams and columns are IPB340. The UNP140 and IPB340 are hot rolled European steel sections with the properties as below:

UNP 140 (channel section): $d = 14$, $A = 20.4$, $I_x = 605$, $I_y = 62.7$.

IPB 340 (wide flange I-shape section): $d = 34$, $A = 171$, $I_x = 36660$, $I_y = 9690$.

where d is depth (cm), A is area (cm²) and I_x and I_y are moments of inertia respectively about x and y axes (cm⁴).

Boundary conditions of finite element model were similar to assumptions of Nast *et al.* (1999) and Walbridge *et al.* (2005). As shown in Fig. 4, the nodes at the intersection of the beam and column were fully restrained in all six degrees of freedom. One end of the brace member was connected to the splice member, and the other end was restrained from out of plane translation, and free in all other degrees of freedom. The gusset plate was welded to the beam and column and connected to the bracing using a splice plate with bolted connections. The bolts were modelled using Abaqus Spring2 elements as flexible links (springs) between the gusset plate and the splice members. This spring element links a global degree of freedom at one node with a global degree of freedom at another node. For this model, for each inplane displacement degree of freedom, one spring was required. The location of the bolt links are shown in Fig. 4. Use of elastic fastener model for bolts (flexible links) doesn't have significant effect on the load vs. out of plane displacement behaviour of gusset plate and has little effect on the ultimate load. Then rigid bolt model and flexible bolt condition are similar, therefore each of them can be used in finite element analysis (Walbridge *et al.* 2005).

In the nonlinear buckling analysis, the three factors initial imperfection, eccentricity of axial external loads and existence of lateral loads lead to buckling. In the ideal conditions and the theoretical environment of the software, without the factors above the buckling does not occur. In practical cases, however, small values of these parameters always exist. Actual members always have imperfections, both in the way the load is applied (eccentricity or inclination with respect to the axis) and with respect to the geometry of the member (residual curvature, non-constant cross-section, etc.). Therefore, in order to calculate the nonlinear buckling capacity of a plate,

consideration of at least one of the parameters above in the analyses is necessary. Use of initial imperfection is common in buckling analysis of plates. This initial imperfection is normally assumed to be similar to the buckled shape, and can be considered as a small coefficient of buckling mode shapes. This small coefficient is assumed to be fraction of the plate thickness or plate width (for example 25% of the plate thickness or 0.05% of the plate width) (Walbridges *et al.* 1998 and El-Sawy *et al.* 2004).

To estimate the critical buckling loads of ideal structures, eigenvalue buckling analysis is generally used. In an eigenvalue buckling problem, the loads for which the stiffness matrix of the model becomes singular are searched. In this research, at first the linear buckling analysis (eigenvalues method) is done by defining the first five buckling modes. The eigen values of buckling for different modes are calculated. The obtained values show that the first, second and third modes are controller. Then, exerting imperfection in the plate by the method of applying small coefficients in the combination of all deformations caused by linear buckling, the first geometrical model for non-linear buckling analysis is calculated. Finally, by defining the RIKS analysis method in the software, the applied load starts from zero and is increased step by step till

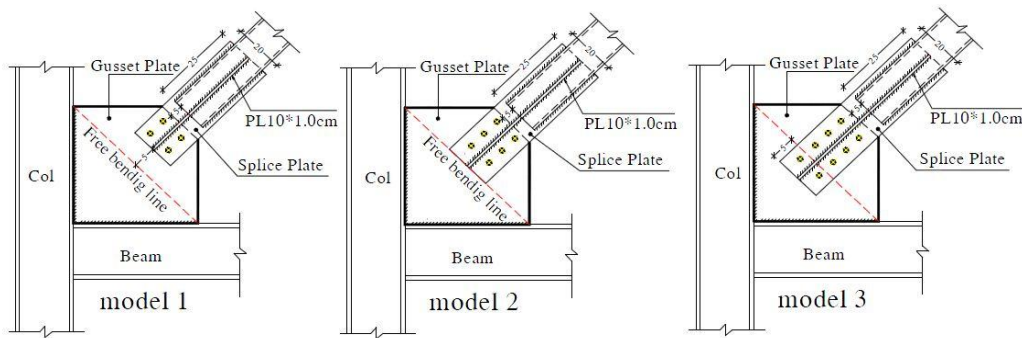


Fig. 3 The position of gusset plates before, over and after the free bending line

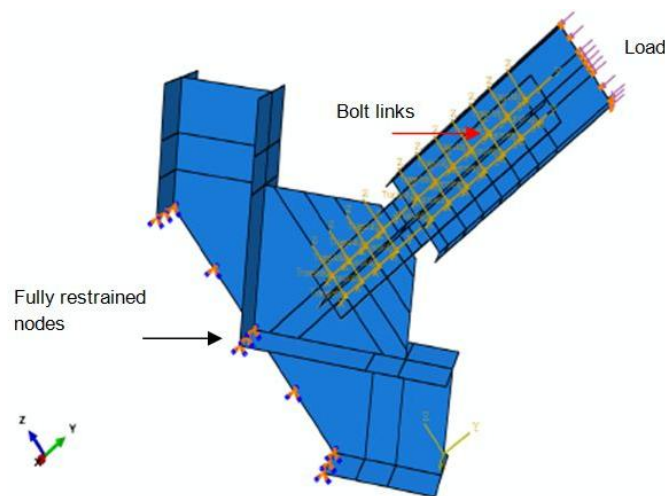


Fig. 4 Loading and boundary conditions for finite element model

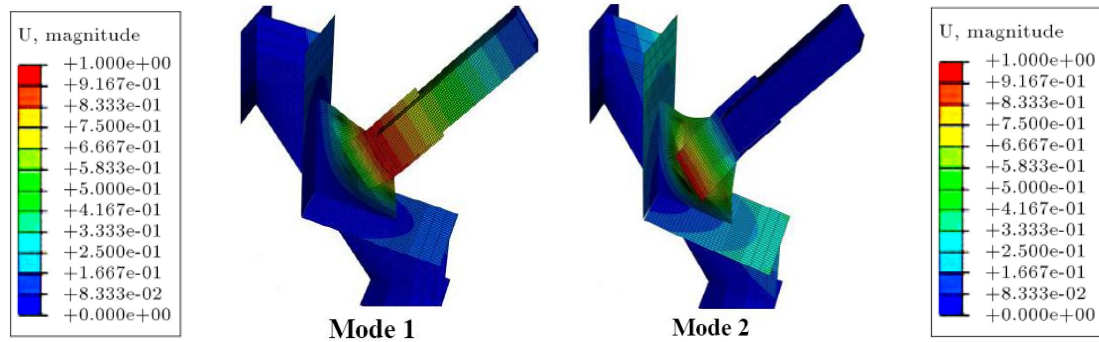


Fig. 5 Buckling deformation of gusset plate

buckling is achieved. Since the loading magnitude is part of the solution, a maximum value of the load proportionality factor, or a maximum displacement value at a specified degree of freedom can be used as stopping criterion. The step will finish when either value is crossed. If neither of these finishing conditions is specified, the analysis will continue for the number of increments specified in the step definition. This method is applicable for studying the buckling and post-buckling behavior of gusset plates.

In Fig. 5, two buckling modes of the gusset plate is shown. Buckling mode 1 occurs to the splice plate in the distance between the gusset plate and the bracing. In mode 2 of buckling, the splice plate in the gap moves outward and causes buckling at the end of the splice plate.

It should be stated that all members are modeled using four-node shell elements, each node having six degrees of freedom. A relatively fine mesh (25 mm by 25 mm) was used near gusset plate connection according to recommendation of Lehman *et al.* (2008). A coarser mesh was used elsewhere, where only limited plastic deformations were expected. By changing the mesh size, the accuracy of modeling and mesh dependency were controlled. The final mesh size had enough accuracy and was according to Roeder *et al.* (2004) and Lehman *et al.* (2008) considerations.

3. Evaluating the accuracy of modeling

For evaluating the accuracy of modeling, the results from Yam and Cheng (1993, 2002) laboratory tests were used. The laboratory model measures the compressive capacity of corner gusset plates under uniform compressive loads. Yam and Cheng considered the effect of plate dimensions and thickness, bracing angle, and the effect of end moment of beams and columns on the buckling capacity of the gusset plate. Their laboratory results showed that by increasing the thickness or decreasing dimensions of the gusset plate, the buckling capacity improves and also the bracing angle and end moments of beams and columns do not have any impact on the buckling load. In Fig. 6 the laboratory model of Yam and Cheng along with the finite element model are shown. Table 1 represents a comparison between the results of two laboratory models GP2 and GP3 of Yam and Cheng with those acquired from the numerical simulation. The error level of the numerical method for estimation of critical load is less than 6%, which shows adequate accuracy of the numerical modeling. Also, pushover curves of non-linear analysis for GP2 and GP3 specimens are provided in Figs. 7(a) and (b) to compare the results of numerical finite element (FE) method and the experimental model. Also in these figures FE results of this study are compared

Table 1 Description of the experimental model

Specimen	Column & beam section	Brace section	Gusset plate dimensions (cm)	Splice plate dimensions (cm)	Ultimate load (Experimental)	Ultimate load (Numerical)	Error percentage
GP2	W310*129	W250*67	PL50*40*0.98	2PL87*14.8*1.3	1356 KN	1435 KN	5.82
GP3	W310*129	W250*67	PL50*40*0.65	2PL87*14.8*1.3	742KN	719 KN	3.10

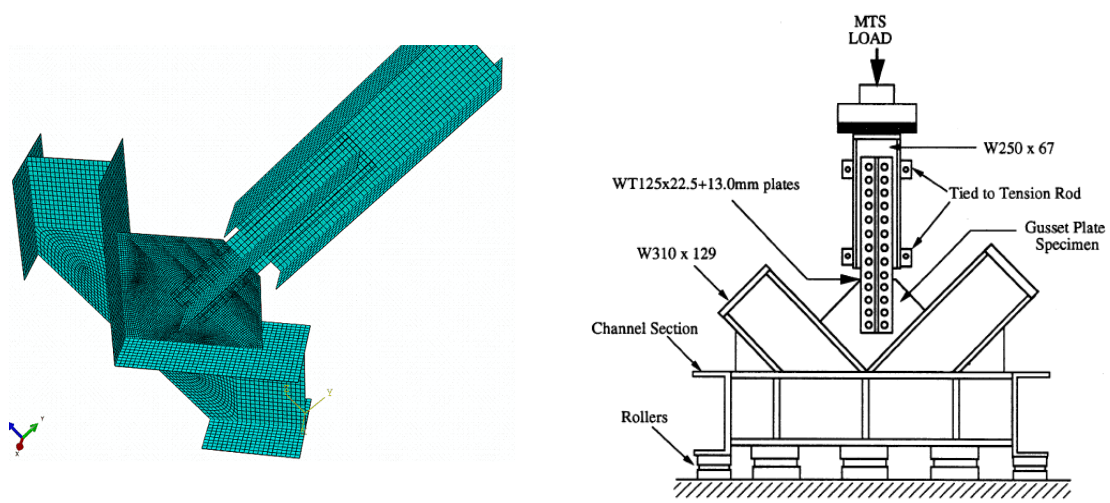
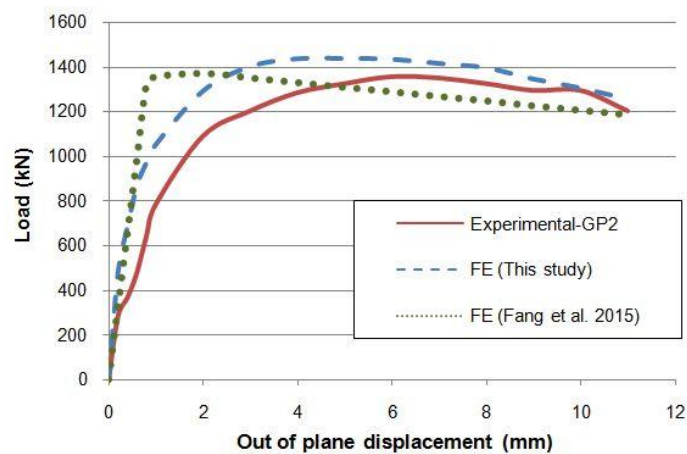
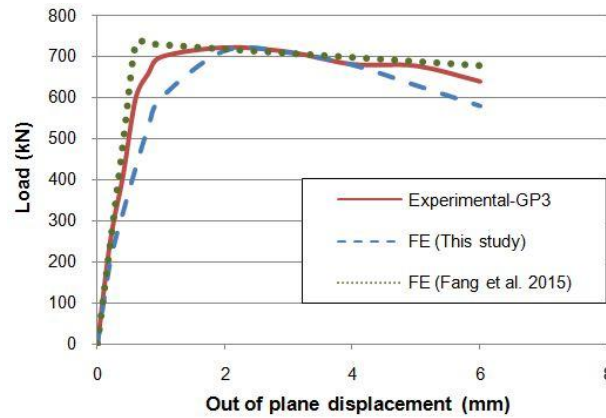


Fig. 6 Experimental and numerical models of bracing gusset plate based on Yam and Cheng (2002) studies



(a) Specimen GP2

Fig. 7 The pushover curve for comparing the numerical modeling results with Yam and Cheng (2002) experimental results



(b) Specimen GP3

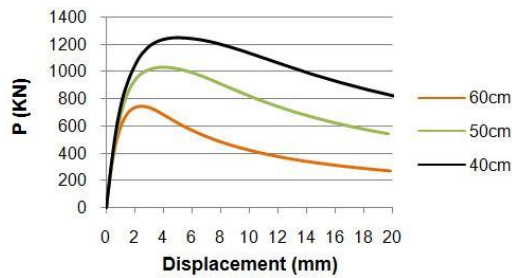
Fig. 7 Continued

with FE results of Fang *et al.* (2015). By comparing the numerical model against the test results, it is observed that the critical load and general trend of the load–displacement curve can be well predicted by the finite element models. However, the initial slope of the FE curves is different the test curves. In other words, the actual out-of-plane displacements of the test specimens are different the FE predictions at initial loading stages. It can also be seen in the works of other researchers such as Fang *et al.* (2015). This may be due to the sensitivity of the FE models to the initial imperfections. The ultimate load and initial load– displacement stiffness (slope) decrease with increasing initial imperfection amplitudes. In addition, boundary condition of the bracing member in the FE analysis was slightly different with the test. In the FE analysis a fully laterally restrained condition was assumed for the bracing member. But, in the tests, the diagonal bracing member was designed to be fixed in place by only four tension rods bolted to a set of columns located at 4 m away from the test frame. In this case, minor movement of the bracing member could occur due to the flexibility of the lateral restraining device using the tension rods (Fang *et al.* 2015).

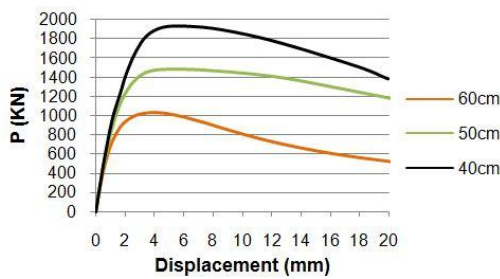
4. Numerical studies

4.1 The influence of gusset plate dimension

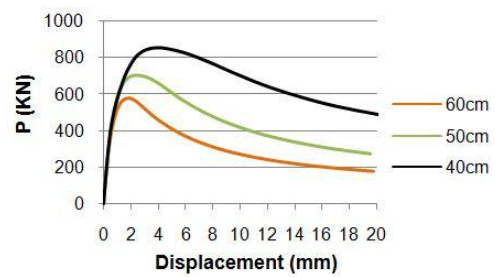
For different dimensions of gusset plate, 40×40, 50×50 and 60×60 cm with a thickness of 15 mm, buckling and post buckling behavior graphs are shown in Fig. 8. As shown in the graphs, after buckling of the gusset plate, the compression capacity of the plate reduces and deformation of the plate increases. Also, these diagrams show that by increasing the dimension of the gusset plate, buckling capacity decreases. Since the lateral stiffness of the gusset plate decreases by increasing the dimension, in cases with larger dimensions failure due to instability usually controls the plate behavior. As shows in Fig. 8, when the bracing passes the bending free line, no considerable change is seen in post buckling capacity of the gusset plate after reaching the maximum compressive capacity. But, when the bracing is on or before the free bending line, the decrease in the capacity of the gusset plate after critical buckling is more visible.



(a) Position of bracing on the free bending line

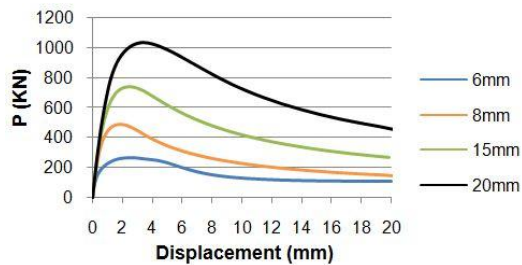


(b) Position of bracing after the free bending line

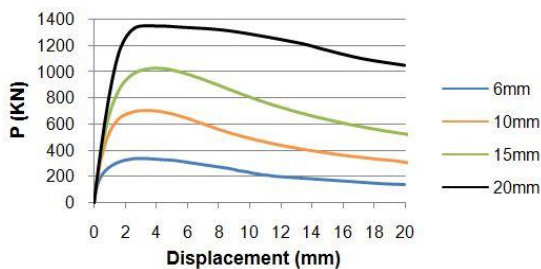


(c) Position of bracing before the free bending line

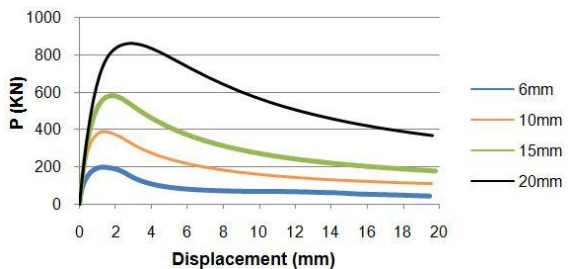
Fig. 8 The influence of dimension on buckling and post buckling behavior of the bracing gusset plate with 15 mm thickness



(a) Position of bracing on the free bending line



(b) Position of bracing after the free bending line



(c) Position of bracing before the free bending line

Fig. 9 The influence of thickness on buckling and post buckling behavior of the gusset plate with 60×60 cm dimension

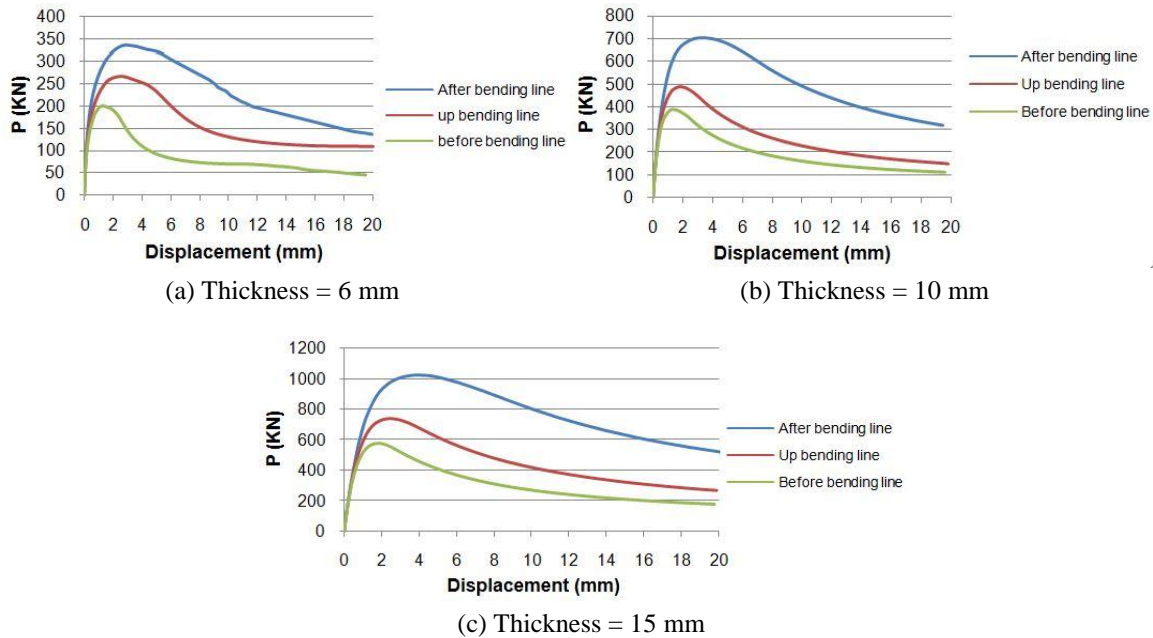


Fig. 10 The influence of the position of bracing splice plate on buckling and post buckling behavior of gusset plate with 60×60 cm dimension

4.2 The influence of thickness of gusset plate

From the diagrams drawn for different thicknesses of 6, 10, 15 and 20 mm of the gusset plate with dimension of 60×60 cm, as shown in Fig. 9, it is clear that by increasing the thickness of the gusset plate, buckling capacity of the plate increases.

4.3 The influence of position of bracing with respect to the free bending line

From the diagrams shown in Fig. 10, it is clear that by increasing the length of the bracing splice plate and passing it from the free bending line, the lateral support will increase the out-of-plane stiffness of the gusset plate and therefore the compressive strength of the plate will increase. In addition, in the models in which the splice plate passes the free bending line, the post buckling behavior is better than other models. This post buckling response of the gusset plate can improve the characteristic of energy absorption and will show proper behavior under applied loads. Also, if the splice plate stands before the free bending line, e.g., in thin plates, a severe decrease in post buckling strength will be seen. As can be seen in Figs. 8-10, until the gusset plate does not reach the critical load, the load-deformation diagram is nearly linear, and the deformation in the gusset plate is very small.

5. Comparing the numerical analysis results with those of Whitmore, Thornton and Modified Thornton methods

In Tables 2, 3 and 4, comparisons of the numerical results of buckling load of the gusset plate

connections with Whitmore's method (Whitmore 1952), Thornton's method (Thornton 1984) and Modified Thornton's method (Yam and Cheng 1993) are shown. In these tables the Whitmore load is obtained from the following formula

$$R_n = A_w \cdot F_y \tag{1}$$

where R_n is the nominal capacity, A_w is effective area, and F_y is the yielding stress of the gusset plate. In Thornton's (1984) method, buckling load of the gusset plate is assumed to be equal to the compressive strength of column strip with effective width of Whitmore (b_E) and fixed-end supports. Thornton's formula for determining the critical buckling load is as follows

$$P_n = A_g \cdot F_{cr} \tag{2}$$

$$\lambda c = \frac{KL_c}{r\pi} \sqrt{\frac{F_y}{E}} \tag{3}$$

$$\lambda c < 1.5 \rightarrow F_{cr} = (0.658\lambda_c^2)F_y \tag{4}$$

$$\lambda c > 1.5 \rightarrow F_{cr} = \left[\frac{0.877}{\lambda_c^2} \right] \cdot F_y \tag{5}$$

where P_n is the ultimate compressive strength of the member, A_g is Whitmore's effective area, F_{cr} is the critical compressive stress, L_c is effective length, K is effective length factor, E is elastic modulus, r is radius of gyration and F_y defines the yielding stress of gusset plate.

As seen on the tables, the results of these approximate methods are only under special conditions close to those from the finite element method, and hence cannot be used for any dimensions or thicknesses accurately, and thus depend strictly on the position of the bracing on the gusset plate. Somehow, by inserting the bracing before the free bending line, buckling loads calculated using these methods would be much more different from those through numerical analysis.

Table 2 Comparison of numerical loads with Whitmore, Thornton and Modified Thornton loads (Position of splice plate is after the free-bending line)

Gusset plate dimension (cm)	$P_{Whitmore}$ (KN)	$P_{Thornton}$ (KN)	$P_{Modified Thornton}$ (KN)	$P_{Numerical}$ (KN)	$\frac{P_{Numerical}}{P_{Whitmore}}$	$\frac{P_{Numerical}}{P_{Thornton}}$	$\frac{P_{Numerical}}{P_{Modified Thornton}}$
60*60*0.6	518.4	175.4	263.2	334.0	0.64	1.90	1.27
60*60*0.8	1152.0	424.3	636.5	510.0	0.44	1.20	0.80
60*60*1.0	1440.0	797.0	1195.4	702.0	0.49	0.88	0.59
60*60*1.2	1728.0	1145.0	1717.5	878.0	0.51	0.77	0.51
60*60*1.5	2160.0	1641.0	2461.4	1027.0	0.48	0.63	0.42
40*40*0.6	561.6	307.8	449.9	592.0	1.05	1.92	1.32
40*40*0.8	748.8	531.1	797.3	887.0	1.18	1.67	1.11
40*40*1.0	936.0	742.1	1124.0	1277.0	1.36	1.72	1.14

Table 2 Continued

Gusset plate dimension (cm)	$P_{Whitmore}$ (KN)	$P_{Thornton}$ (KN)	$P_{Modified Thornton}$ (KN)	$P_{Numerical}$ (KN)	$\frac{P_{Numerical}}{P_{Whitmore}}$	$\frac{P_{Numerical}}{P_{Thornton}}$	$\frac{P_{Numerical}}{P_{Modified Thornton}}$
40*40*1.2	1123.2	946.9	1440.6	1574.0	1.40	1.66	1.09
40*40*1.5	1404.0	1247.6	1904.9	1919.0	1.37	1.54	1.01
60*48*0.6	842.4	223.2	354.8	385.0	0.46	1.73	1.09
60*48*0.8	1123.2	537.2	854.0	591.0	0.53	1.10	0.69
60*48*1.0	1404.0	885.8	1408.2	809.0	0.58	0.91	0.57
60*48*1.2	1684.8	1213.9	1929.8	1003.0	0.60	0.83	0.52
60*48*1.5	2106.0	1686.5	2681.1	1289.0	0.61	0.76	0.48
40*32*0.6	561.6	307.8	473.5	640.0	1.14	2.08	1.35
40*32*0.8	748.8	531.1	817.0	1056.0	1.41	1.99	1.29
40*32*1.0	936.0	742.1	1141.6	1419.0	1.52	1.91	1.24
40*32*1.2	1123.2	946.9	1456.7	1695.0	1.51	1.79	1.16
40*32*1.5	1404.0	1247.6	1919.4	2297.0	1.64	1.84	1.20

Table 3 Comparison of numerical loads with Whitmore, Thornton and Modified Thornton loads
(Position of splice plate is on the free-bending line)

Gusset plate dimension (cm)	$P_{Whitmore}$ (KN)	$P_{Thornton}$ (KN)	$P_{Modified Thornton}$ (KN)	$P_{Numerical}$ (KN)	$\frac{P_{Numerical}}{P_{Whitmore}}$	$\frac{P_{Numerical}}{P_{Thornton}}$	$\frac{P_{Numerical}}{P_{Modified Thornton}}$
60*60*0.6	712.8	117.8	179.5	266.0	0.37	2.26	1.48
60*60*0.8	950.4	279.6	423.6	380.0	0.40	1.36	0.90
60*60*1.0	1188.0	557.9	845.3	487.0	0.41	0.87	0.58
60*60*1.2	1425.6	856.3	1297.4	667.0	0.47	0.78	0.51
60*60*1.5	1782.0	1275.9	1933.2	741.0	0.42	0.58	0.38
40*40*0.6	561.6	307.8	449.9	338.0	1.05	1.92	1.32
40*40*0.8	748.8	531.1	797.3	578.0	1.18	1.67	1.11
40*40*1.0	936.0	742.1	1124.0	783.0	1.36	1.72	1.14
40*40*1.2	1123.2	946.9	1440.6	1033.0	1.40	1.66	1.09
40*40*1.5	1404.0	1247.6	1904.9	1249.0	1.37	1.54	1.01
60*48*0.6	842.4	223.2	354.8	313.0	0.46	1.73	1.09
60*48*0.8	1123.2	537.2	854.0	485.0	0.53	1.10	0.69
60*48*1.0	1404.0	885.8	1408.2	689.0	0.58	0.91	0.57
60*48*1.2	1684.8	1213.9	1929.8	825.0	0.60	0.83	0.52
60*48*1.5	2106.0	1686.5	2681.1	1002.0	0.61	0.76	0.48
40*32*0.6	561.6	307.8	473.5	382.0	1.14	2.08	1.35
40*32*0.8	748.8	531.1	817.0	670.0	1.41	1.99	1.29
40*32*1.0	936.0	742.1	1141.6	961.0	1.52	1.91	1.24
40*32*1.2	1123.2	946.9	1456.7	1178.0	1.51	1.79	1.16
40*32*1.5	1404.0	1247.6	1919.4	1407.0	1.64	1.84	1.20

Table 4 Comparison of numerical loads with Whitmore, Thornton and Modified Thornton loads
(Position of splice plate is before the free-bending line)

Gusset plate dimension (cm)	P _{Whitmore} (KN)	P _{Thornton} (KN)	P _{Modified Thornton} (KN)	P _{Numerical} (KN)	$\frac{P_{\text{Numerical}}}{P_{\text{Whitmore}}}$	$\frac{P_{\text{Numerical}}}{P_{\text{Thornton}}}$	$\frac{P_{\text{Numerical}}}{P_{\text{Modified Thornton}}}$
60*60*0.6	583.2	79.0	117.5	188.0	0.32	2.38	1.60
60*60*0.8	777.6	189.1	280.2	296.0	0.38	1.57	1.06
60*60*1.0	972.0	367.2	550.8	467.0	0.48	1.27	0.85
60*60*1.2	1166.4	623.4	923.6	504.0	0.43	0.81	0.55
60*60*1.5	1458.0	976.5	1446.7	741.0	0.51	0.76	0.51
40*40*0.6	345.6	97.1	121.0	236.0	0.68	2.43	1.95
40*40*0.8	460.8	230.3	287.8	346.0	0.75	1.50	1.20
40*40*1.0	576.0	371.9	464.9	513.0	0.89	1.38	1.10
40*40*1.2	691.2	505.7	632.1	647.0	0.94	1.28	1.02
40*40*1.5	864.0	698.7	873.4	863.0	1.00	1.24	0.99
60*48*0.6	604.8	100.5	150.8	206.0	0.34	2.05	1.37
60*48*0.8	806.4	237.2	355.9	311.0	0.39	1.31	0.87
60*48*1.0	1008.0	473.4	710.0	504.0	0.50	1.06	0.71
60*48*1.2	1209.6	726.6	1089.8	572.0	0.47	0.79	0.52
60*48*1.5	1512.0	1082.6	1623.9	789.0	0.52	0.73	0.49
40*32*0.6	324.0	113.7	144.0	268.0	0.83	2.36	1.86
40*32*0.8	432.0	251.1	318.1	492.0	1.14	1.96	1.55
40*32*1.0	540.0	379.3	480.5	716.0	1.33	1.89	1.49
40*32*1.2	648.0	501.8	635.6	940.0	1.45	1.87	1.48
40*32*1.5	810.0	679.8	861.1	1131.0	1.40	1.66	1.31

6. Presenting design diagrams

Simplified methods such as Whitmore, Thornton and Modified-Thornton are approximate procedures to calculate the capacity of gusset plates. In such methods, effects of some parameters such as the position of the bracing member with respect to the free bending line, the length-to-width ratio of the gusset plate, etc. are not considered. Thus, these methods do not have adequate accuracy for some problems.

A more accurate method was proposed by Sheng *et al.* (2002). In this method, instead of using a column buckling equation for estimating the ultimate load of the plate, another design method based on the inelastic critical buckling stress of plate is proposed. The suggested equations for calculating the buckling capacity of gusset plate are as follows

$$P_U = \sigma_U \cdot b_1 \cdot t \tag{6}$$

$$\sigma_u = \frac{K_g \pi^2 E \sqrt{\frac{E_t}{E}}}{12 (1 - \nu^2) \left(\frac{b_0}{t}\right)^2} \tag{7}$$

where P_u is buckling capacity of the plate, σ_u is elastic critical buckling stress, b_1 is the length of free bending line, t is thickness of the plate, E is elastic modulus, ν is Poisson's ratio, b_0 is length of the shorter side of the gusset plate, $E = 50E_t$ and K_g is a constant factor that relates to the ratio of length to wide of the plate, type of stress, the plate's edge support condition and the position of the bracing on the gusset plate.

In the research conducted by Sheng *et al.* (2002), only 3 different thicknesses and dimensions have been used. These selected dimensions are good for research purposes but executive purposes have not been taken into account. In this paper, different practical thicknesses and dimensions of the gusset plate have been considered. The buckling load of the gusset plate is calculated using a finite element software program ($P_{software}$). By substituting this calculated load into Eq. (8), the value of K_g is obtained. Design diagrams for the K_g factor for different thicknesses and dimensions of gusset plate and also for different positions of the bracing relative to the free bending line are drawn and presented in Figs. 11-13

$$K_g = \frac{12(1 - \nu^2) \left(\frac{b_0}{t}\right)^2 P_{software}}{\pi^2 E \sqrt{\frac{E_t}{E}}} * \frac{1}{b_1 \cdot t} \tag{8}$$

Therefore, instead of using the methods provided by AISC (2001) regulations such as Whitmore (1952) and Thornton (1984), in order to determine the buckling load of the gusset plate, the value of K_g factor will be obtained from one of the diagrams in Figs. 11-12 or 13. Then, the inelastic critical buckling stress and buckling load of the gusset plate can be calculated respectively from Eqs. (7) and (6). For example, for a plate with 50×40×1.0 cm dimension, if the bracing stands after the free bending line, the amount of K_g according to the diagram of Fig. 11 is 11.3, and by substituting it into Eqs. (7) and (6) the amount of buckling load for the gusset plate equals 1213 kN.

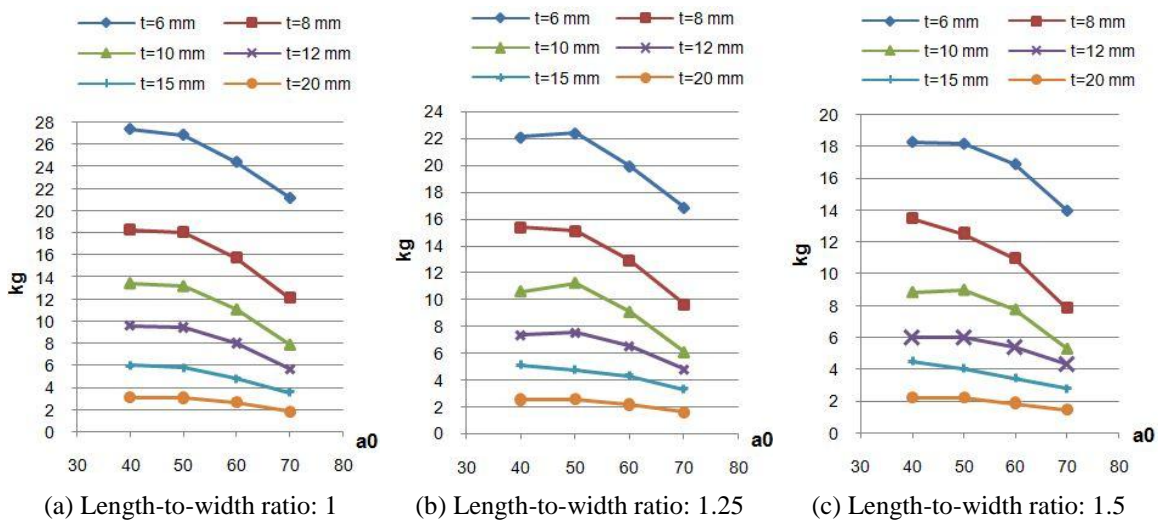


Fig. 11 The Kg factor based on the position of splice plate after the free bending line

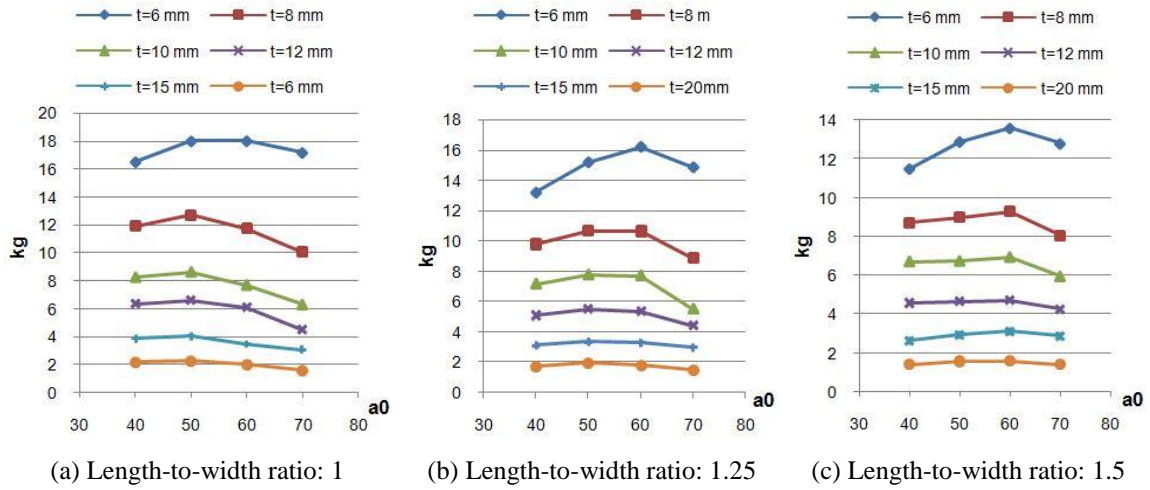


Fig. 12 The Kg factor based on the position of splice plate on the free bending line

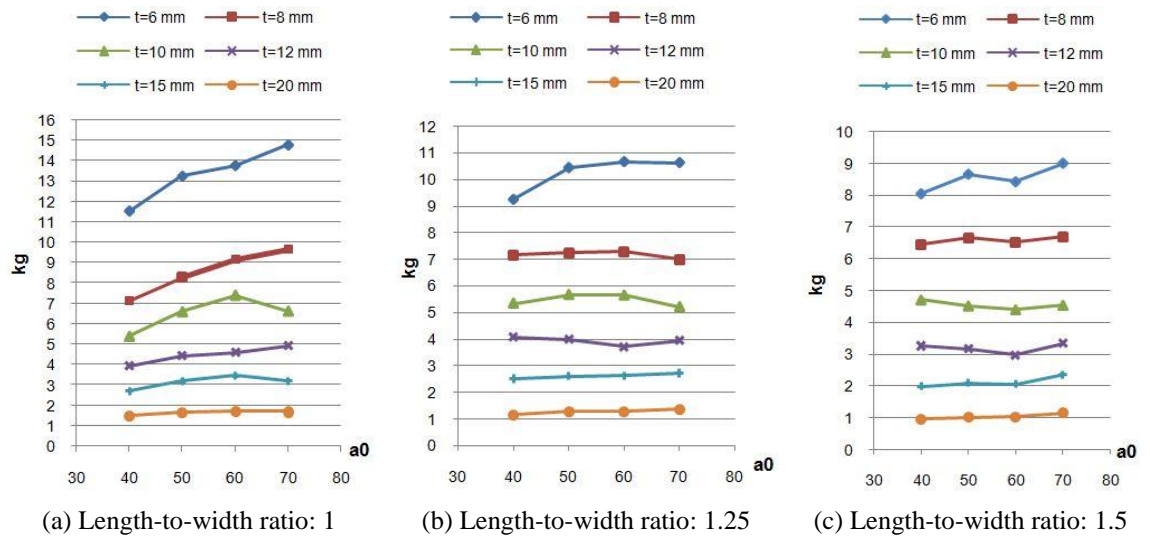


Fig. 13 The Kg factor based on the position of splice plate before the free bending line

Table 5 Comparison of buckling capacity of PL 40×40×1.0 cm between Sheng *et al.* (2002) method and the proposed numerical method

Position of bracing	K_g	σ_u (N/cm ²)	P_{Sheng} (kN)	$P_{Numerical}$ (kN)	Error percentage
After free bending line	13.6	22792	1287	1277	0.8
On the free bending line	8.2	13742	776	783	0.9
Before free bending line	5.3	8882	502	513	2.1

In the mentioned diagrams, the horizontal axis shows the longer dimension of the gusset plate in millimeters (a_0) and the vertical shows the K_g factor. Design diagrams are based on the rectangular gusset plate and for using other shapes, new graphs can be developed.

In Table 5, the results of the proposed numerical model for buckling capacities of PL 40×40×1.0 cm at different positions of the bracing with respect to the free bending line are compared with the results of Sheng *et al.* method (2002), that shows great accuracy of the proposed approach.

7. Conclusions

The results acquired from the numerical analysis of the models are as follows:

- Position of bracing splice plate after the free bending line only increases the buckling capacity of the gusset plate and does not have any considerable influence on post buckling capacity of the gusset plate after reaching the maximum compressive capacity, and the plate doesn't show much ductility.
- By increasing the thickness and decreasing dimensions of bracing gusset plate, the buckling capacity of the plate increases.
- If the bracing stands before the free bending line, the post buckling strength of thin plates decreases extremely.
- In all models before reaching the critical load, the load-displacement diagram is linear and the deformation in the gusset plate is not considerable.
- Whitmore and Thornton methods are simplified and approximate methods and for some problems these methods do not have adequate accuracy. The use of such methods depends on the position of the bracing on the gusset plate.
- To determine the accurate buckling load of the gusset plate, instead of using common procedures of codes, the factor k_g and the proposed graphs of this paper can be used.
- By increasing the bracing splice length so that it passes the free bending line, the factor K_g increases, and eventually the buckling capacity of the plate increases.
- By increasing the length-to-width ratio of the gusset plate, the amount of K_g decreases and therefore the buckling capacity of the plate decreases.

References

- AISC (2001), Manual of steel construction load and resistance factor design; (3rd Edition), American Institute of Steel Construction, Chicago, IL, USA.
- AISC (2005), Seismic provisions for structural steel buildings; American Institute of Steel Construction, Chicago, IL, USA.
- Astaneh-Asl (1998), Seismic behavior and design of gusset plates; Structural Steel Educational Council.
- Bazzaz, M., Kheyroddin, A., Kafi, M.A. and Andalib, Z. (2012), "Evaluation of the seismic performance of off-center bracing system with ductile element in steel frames", *Steel Compos. Struct., Int. J.*, **12**(5), 445-464.
- Chen, S.J. and Chang, C.C. (2012), "Experimental study of low yield point steel gusset plate connections", *J. Thin-Wall. Struct.*, **57**, 62-69.
- Crosti, C. and Duthinh, D. (2014), "A nonlinear model for gusset plate connections", *Eng. Struct.*, **62**, 135-147.
- Deliktas, B. and Mizamkhan, A. (2014), "Modeling nonlinear behavior of gusset plates in the truss based

- steel bridges”, *Struct. Eng. Mech., Int. J.*, **51**(5), 809-821.
- El-Sawy, K.M., Nazmy, A.S. and Martini, M.I. (2004), “Elasto-plastic buckling of perforated plates under uniaxial compression”, *Thin-Wall. Struct.*, **42**(8), 1083-1101.
- Fang, C., Yam, M.C.H., Cheng, J.J.R. and Zhang, Y. (2015), “Compressive strength and behaviour of gusset plate connections with single-sided splice members”, *J. Construct. Steel Research*, **106**, 166-183.
- Gross, J.L. (1990), “Experimental study of gusseted connections”, *Eng. J., AISC*, **27**(3), 89-97.
- Güneyisi, E.M. and Ameen, N. (2014), “Structural behavior of conventional and buckling restrained braced frames subjected to near-field ground motions”, *Earthq. Struct., Int. J.*, **7**(4), 553-570.
- Hadianfard, M.A., Khakzad, A.R. and Vaghefi, M. (2015), “Analysis of the effect of stiffener on the buckling capacity and non-elastic behavior of bracing gusset plates”, *Scientia Iranica*, Transaction A, Civil Engineering, **22**(4), 1449-1456.
- Hashemi, H., Behnamfar, B.F. and Ranjbaran, F. (2008), “Effects of local eccentricity of connecting braces on nonlinear behavior of steel concentric brace connections”, *J. Seismol. Earthq. Eng.*, **10**(2), 91-99.
- Hassan, M.M., Ramadan, H.M., Naeem, M. and Mourad, S.A. (2014), “Behavior of gusset plate-to-CCFT connections with different configurations”, *Steel Compos. Struct., Int. J.*, **17**(5), 735-751.
- Lehman, D.E., Roeder, C.W., Herman, D., Johnson, S. and Kotulka, B. (2008), “Improved seismic performance of gusset plate connections”, *J. Struct. Eng.*, **134**(6), 890-901.
- Lutz, D.G. and LaBoube, R.A. (2005), “Behavior of thin gusset plates in compression”, *Thin-Wall. Struct.*, **43**, 861-875.
- Naghipour, M., Abdollahzadeh, G. and Shokri, M. (2013), “Analysis and design procedure of corner gusset plate connection in BRBFs”, *Iranica J. Energy Environ.*, **4**(3), 271-282.
- Nast, T.E., Grondin, G.Y. and Cheng, J.R. (1999), “Cyclic behavior of stiffened gusset plate-brace member assemblies”, Structural Eng. Report No. 229; Department of Civil and Environmental Engineering, University of Alberta, AL, USA.
- Rabinovitch, J.S. and Cheng, J.J.R. (1993), Cyclic behaviour of steel gusset plate connections, Structural Eng. Report No. 191; University of Alberta, AL, USA.
- Rajasekaran, S. and Wilson, A.J. (2013), “Buckling and vibration of rectangular plates of variable thickness with different end conditions by finite difference technique”, *Struct. Eng. Mech., Int. J.*, **46**(2), 269-294.
- Roeder, C.W., Lehman, D.E. and Yoo, J.H. (2004), “Performance based seismic design of braced-frame connections”, *Proceedings of the 7th Pacific Structural Steel Conference*, Long Beach, CA, USA, March.
- Sheng, N., Yam, C.H. and Iu, V.P. (2002), “Analytical investigation and the design of the compressive strength of steel gusset plate connections”, *J. Construct. Steel Res.*, **58**, 1473-1493.
- Thornton, W.A. (1984), “Bracing connections for heavy construction”, *Eng. J., AISC*, **21**(3), 139-148.
- Walbridge, S.S., Grondin, G.Y. and Cheng, J.J.R. (1998), “An analytical study of the cyclic behaviour of steel gusset plate connections”, *Annual Conference of the Canadian Society for Civil Engineering (CSCE)*, Halifax, NS, Canada, June, pp. 107-116.
- Walbridge, S.S., Grondin, G.Y. and Cheng, J.J. (2005), “Gusset plate connections under monotonic and cyclic loading”, *Can. J. Civil Eng.*, **32**(5), 981-995.
- Whitmore, R.E. (1952), Experimental investigation of stresses in gusset plates, Bulletin No. 16, Engineering Experiment Station, University of Tennessee, TN, USA.
- Yam, M.C.H. and Cheng, J.J.R. (1993), “Experimental investigation of the compressive behaviour of gusset plate connections”, Structural Engineering Report No. 194; University of Alberta, AL, USA.
- Yam, M.C.H. and Cheng, J.J.R. (2002), “Behavior and design of gusset plate connections in compression”, *J. Construct. Steel Res.*, **58**(5-8), 1143-1159.